Editors' Suggestion

Phase-Variation Ramsey Spectroscopy of the $2^3S_1 \rightarrow 2^3P_2$ Interval in Positronium

D. M. Newson and D. B. Cassidy
Department of Physics and Astronomy, University College London, Gower Street, London, WC1E 6BT, United Kingdom

(Received 7 October 2025; accepted 2 January 2026; published 22 January 2026)

The $2\,^3S_1 \rightarrow 2\,^3P_2$ interval (ν_2) in positronium has been measured using a phase-variation separated oscillatory fields technique. A beam of positronium atoms in the $2\,^3S_1$ state was passed through two spatially separated coherent microwave fields tuned close to the ν_2 resonance frequency (8626.71 ± 0.08 MHz), and the surviving beam fraction was recorded as a function of the relative phase between the fields. The resonance frequency was obtained from the frequency dependence of the phase of the interference signal without scanning over the full spectral line shape of the transition. We obtain $\nu_2 = 8626.39 \pm 1.17_{\text{stat}} \pm 0.80_{\text{sys}}$ MHz, which is in agreement with QED theory.

DOI: 10.1103/f2m8-5zxj

As a leptonic atom with negligible weak force contributions [1], positronium (Ps), the electron-positron bound state, is almost entirely described by bound-state quantum electrodynamics (QED) theory [2]. This means Ps is an ideal system with which to test QED theory, and in principle, such tests could be sensitive to new physics not currently included in the framework [3]. However, these tests are useful only if experimental measurements can be performed with comparable precision to the corresponding state-of-the-art calculations. QED corrections to Ps energy levels have now been completed up to $\mathcal{O}(m\alpha^6)$ (see Ref. [4] for a summary), and efforts are currently ongoing to compute higher order terms [5,6]. Unfortunately, however, experimental data are typically less precise than theoretical results by (at least) an order of magnitude [4].

Recent experiments intended to improve the experimental precision of the Ps $n = 2$ fine-structure intervals (i.e., $2\,^3S_1 \rightarrow 2\,^3P_J$) have achieved sub-MHz uncertainty, and further improvements are expected [7,8]. However, measurements of this type are in general susceptible to line shape distortions [9] arising from frequency-dependent variations in the applied microwave radiation power [10]. This problem is exacerbated when the driving frequency must be varied over multiples of the ≈50 MHz natural linewidth arising from the short (3.2 ns) radiative lifetime of the 2P levels [11], ultimately limiting the achievable precision of Rabi-type measurements.

One way to mitigate such effects is to use Ramsey spectroscopy, employing separated oscillatory fields (SOFs) [12,13]. This technique involves replacing the single interaction region used in standard Rabi measurements with two spatially (or temporally) separated interaction regions that have a definite phase relationship. A superposition of internal quantum states is generated by the first driving field (here, $2\,^3S_1$ and $2\,^3P_2$ states), which then oscillates at the transition resonance frequency as the atoms evolve through a field-free region for time T, and is subsequently projected onto a final-state (either $2\,^3S_1$ or $2\,^3P_2$) according to the relative phase of the oscillating superposition state and the second driving field.

Ordinarily, in a direct Ramsey SOF measurement, spectral line shapes would be obtained for two relative phase conditions (typically 0 and π radians) and a difference spectrum constructed. The width of the central interference fringe in this case will be $\approx 1/2T$, and so for sufficiently large T the width can be smaller than the natural linewidth. However, the interference signal is still measured as a function of the driving field frequency, and in order to resolve multiple fringes, it may still be necessary to scan over a range several times larger than the natural linewidth. In an alternative approach, Klein *et al.* [14] describe a phase-variation SOF (PVSOF) method in which a variable phase difference ϕ is introduced between the two radiation fields. The general form of the SOF interference signal is [15]

$$S \propto A(\Delta, T)\cos(2\pi T\Delta + \phi), \tag{1}$$

where A is a phase-independent amplitude, and $\Delta = (\nu - \nu_0)$ is the detuning from the resonance frequency ν_0. The phase at which S is maximal is $\phi = \phi_{\max} = -2\pi T\Delta$. Thus, by scanning ϕ for different Δ one can find the frequency for which $\phi_{\max} = 0$ with a linear fit. This will correspond to the resonance frequency ν_0 and can be obtained with only a small detuning range. Thus, the PVSOF approach is particularly well suited to Ps

Published by the American Physical Society under the terms of the Creative Commons Attribution 4.0 International license. Further distribution of this work must maintain attribution to the author(s) and the published article's title, journal citation, and DOI.

fine-structure measurements, where many of the systematic effects are related to the need to scan over a large frequency range; specifically, maintaining constant microwave power and splitting the line shape by a large factor ($\gg 100$) [9].

The application of SOF methods to Ps $n = 2$ fine-structure measurements is challenging because atomic superposition states comprising both S and P components typically have very short lifetimes, on the order of 3 ns as dictated by the 2P radiative lifetime. In order to propagate such a beam through two spatially separated waveguides, high velocities and/or small flight distances are required. Standard Ps production methods using thermalized positrons injected into solid-state materials usually result in atoms with energies on the order of 50 meV, corresponding to mean velocities of $\approx 10^5$ ms^{-1} (e.g., [16]). This is compatible with laser excitation techniques, and hence has been the basis for many spectroscopic measurements [17]. However, atoms with these velocities are not suitable for SOF experiments in which the mixed-state lifetimes are on the order of nanoseconds since this would require fields separated by less than a millimeter. Thus, faster $2\,^3S_1$ Ps atoms are required [18]; these can be generated using charge-exchange reactions in a gas cell [19]. Although the Ps formation fraction (i.e., the number of Ps atoms created per incident positron) obtained using this method is small ($\approx 0.1\%$), up to 10% of all Ps atoms produced may be in the $2\,^3S_1$ level, and beam energies up to ≈ 100 eV can be generated [20] which are suitable for SOF measurements.

Here we report a measurement of the $2\,^3S_1 \rightarrow 2\,^3P_2$ interval (8626.71 ± 0.08 MHz [21]) in Ps using the PVSOF method. The experiments were performed using an energetic beam of metastable $2\,^3S_1$ (Ps*) atoms described in detail elsewhere [20]. This beam was generated by passing a magnetically guided positron beam through a Xe gas cell, which produced both ground and excited state Ps atoms. Positrons that passed through the gas cell were removed from the beam by an electric field of strength ≈ 300 V/cm generated by a set of deflector plates. This field is expected to have no effect on Ps atoms and a negligible effect on Ps* atoms, which passed through the deflector and then through two WR-112 microwave waveguides (WG1 and WG2) separated by a distance $d = 17$ mm. The magnetic field strength in the waveguide region was ≈ 40 G, as measured with a Hall probe. After a flight distance of ≈ 540 mm from the gas cell, surviving Ps and Ps* atoms were detected using a 90% open-area microchannel plate detector (MCP), as indicated in Fig. 1.

The Ps* beam energy was set by the incident positron beam energy. This was chosen as a compromise between temporal coherence over the field-free flight time and Ps* production efficiency. The positron beam energy was 78.1 ± 0.9 eV measured using a retarding field analyzer, resulting in a Ps (Ps*) beam energy of 72.8 eV (67.7 eV) [20]. The Ps (Ps*) beam flight time from the gas cell to the detector was approximately 151 ns (157 ns), resulting in 35% (87%) surviving fractions against self annihilation. Since the Ps atoms are unaffected by the applied microwave radiation, these generate a constant background signal. Based on the beam energy distribution and the waveguide geometry and separation, we find an average field-free flight time of $\bar{T} = 4.93 \pm 0.02$ ns, and $\approx 3.65 \pm 0.01$ ns flight time through a single waveguide.

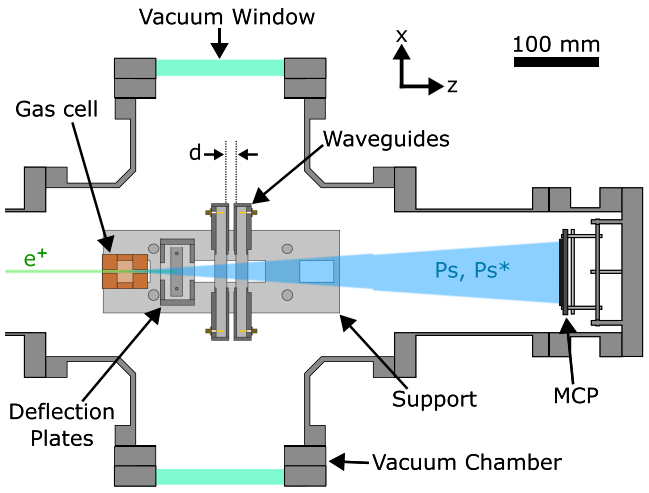


FIG. 1. Top-down scale view of the experimental arrangement showing the vacuum chamber, windows, gas cell, deflection plates, waveguides (WG1, WG2), and MCP detector. The angular divergence of the Ps* beam is represented by the blue shaded region.

The microwave generators and phase control system employed in this Letter are similar to those described in [22]. Briefly, signals with frequency 8611–8641 MHz ($\Delta = \pm 15$ MHz) and power ≈ 20 dBm (100 mW) were generated by two phase-stabilized microwave generators and amplifiers. The output of the amplifiers was connected to the waveguides via coaxial cables, directional couplers, and 40 GHz SMA vacuum feedthroughs. The power (P_c) of the attenuated (−30 dB) and combined outputs from the directional couplers was used to monitor and control the relative phase offset (ϕ) of the microwave radiation in each waveguide.

The waveguides were constructed with closed ends, SMA antenna feeds, and multiple tuning rods set to provide a constant power response ($S_{11} < -30$ dBm measured with a Rhode & Schwarz ZNL4 vector network analyzer (VNA)) over a small frequency range (± 200 MHz) around ν_2. As well as minimizing frequency-dependent power variations, this design completely eliminates reflected microwave radiation within the vacuum chamber, inherent to previous open-ended designs [9], which could result in loss of superposition states and/or dephasing of microwave signals inside the guides. The orientation of the waveguides were such that the oscillating electric field was parallel to the magnetic field, and only $\Delta M_J = 0$ transitions were driven.

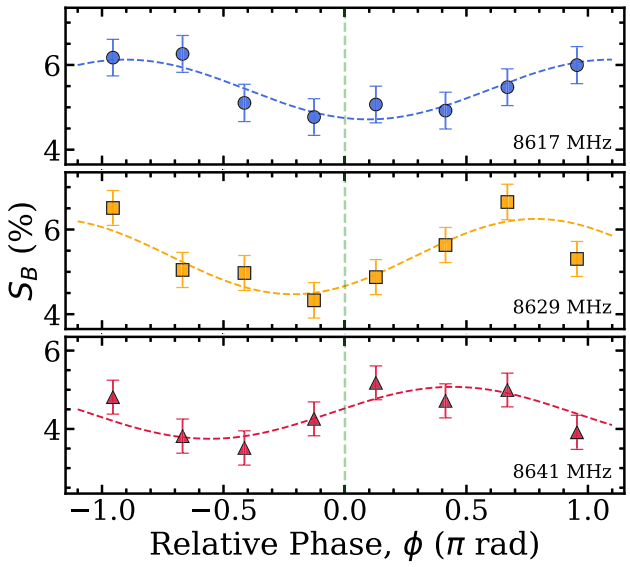


FIG. 2. Measured Ps* signal (S_B) versus relative phase offset (ϕ) for three frequencies close to ν_2. The dashed lines are sinusoidal fits to the data. The error bars indicate statistical uncertainties.

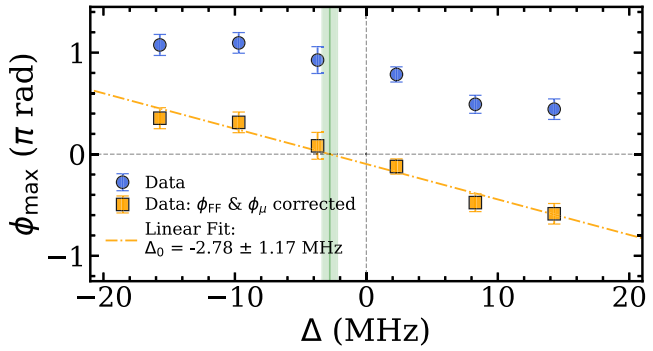


FIG. 3. Modulation phase (ϕ_{max}) versus frequency detuning (Δ) shown with and without the phase corrections applied (see text). The dashed line is a linear fit to the corrected data. The vertical line and shaded region indicate the position and uncertainty of the zero-crossing point (Δ_0) corresponding to the (Zeeman shifted) resonant frequency.

Measuring ν_2 using the PVSOF method relies on recording the fraction of Ps* atoms that reach the detector as ϕ is varied. The relative phase sets the projection of the superposition state onto the short-lived $2\,^3P_2$ state. The latter decays rapidly via fluorescence to the $1\,^3S_1$ ground state, which has a mean annihilation lifetime of 142 ns, a factor of 8 smaller than the $2\,^3S_1$ lifetime (1136 ns). When the radiation experienced by the atoms is in phase (i.e., $\phi = 0$), the projection is maximal and relatively few atoms reach the detector. As ϕ is increased, the surviving fraction increases. This fraction was characterized by the signal parameter (S_B) given by

$$S_B = \frac{S_{\mathrm{OFF}} - S_{\mathrm{ON}}}{S_{\mathrm{OFF}}}, \tag{2}$$

where S_{ON} (S_{OFF}) is the integrated count rate (net of background determined with no gas in the cell) registered by the MCP detector with (without) microwave radiation present in both waveguides.

Figure 2 shows examples of measurements of S_B as a function of ϕ obtained for three frequencies (8617, 8629, and 8641 MHz) close to the expected resonance frequency. The phase of the interference signal was extracted using a sinusoidal fit to the data, and the results are shown versus Δ in Fig. 3. The expected linear dependence of ϕ_{max} with frequency detuning was observed, but the extracted phase is in fact the sum of the interference effect (ϕ_{int}) and systematic contributions such that $\phi_{\mathrm{max}} = \phi_{\mathrm{int}} + \phi_{\mathrm{FF}} + \phi_\mu$. This is because the waveguides were operated with a dominant traveling wave component (rather than a standing wave), so there is an additional phase shift corresponding to the advance of the traveling wave in the second waveguide as the atoms travel through the field-free region. This is given by $\phi_{\mathrm{FF}} = (2\bar{T}\nu \bmod 1) - 1$, where ν is the driving frequency. Using the measured beam energy, we obtain a linear variation of ϕ_{FF} from -0.18 to $0.22\,\pi$rad for frequency detuning between -20 and $+20$ MHz. Additionally, differences in the construction, tuning, and microwave feeds resulted in a fixed relative phase shift ϕ_μ between the waveguides. This was measured directly using a VNA, and varied approximately linearly from 0.86 to 0.87 πrad over the frequency range of interest. These adjustments applied to the measured phase shifts are shown in Fig. 3. With the phase corrections, we obtain a resonance frequency from the zero-crossing point of $\Delta_0 = -2.78 \pm 1.17$ MHz.

The measured detuning offset is primarily due to the Zeeman shift arising from the axial magnetic field in the waveguides. This field was measured to be 41.6 G in WG1 and 36.6 G in WG2 corresponding to Zeeman shifts of -2.77 and -2.14 MHz, respectively [8]. The average Zeeman shift is $\Delta\nu_Z = -2.46$ MHz, and we take the difference as an estimate of the associated systematic error (i.e., 630 kHz). There may also be a Doppler shift if the waveguides are not perfectly aligned with the Ps* beam. Based on the measured alignment of the waveguides and the Xe gas cell alignment, as well as the radial positron and Ps* beam profiles (obtained using a position sensitive detector [20]), we estimate the Doppler shift to be no larger than 500 kHz. In a more precise experiment, this could be explicitly measured using multiple antennas [8]. Contributions from other systematic effects, such as dc, ac, and motional Stark shifts are expected to contribute significantly less than 10 kHz [23]. Therefore, we assign a systematic error of 800 kHz to the measurement. Thus, we obtain a final result for the ν_2 transition frequency of $\nu_2 = 8626.39 \pm 1.17_{\mathrm{stat}} \pm 0.80_{\mathrm{sys}}$ MHz. This result is consistent with QED theory and has a precision that is

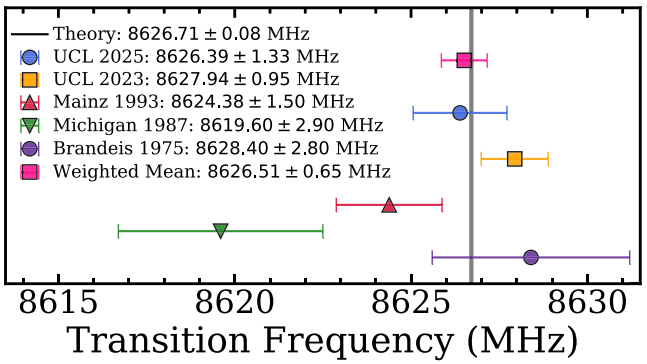


FIG. 4. Comparison of experimentally determined ν_2 transition frequencies with the $\mathcal{O}(m\alpha^6)$ QED calculation [21] (thick vertical line). Statistical and systematic uncertainties of the measured values have been added in quadrature. Also shown is the weighted average of all measurements, which is in good agreement with theory.

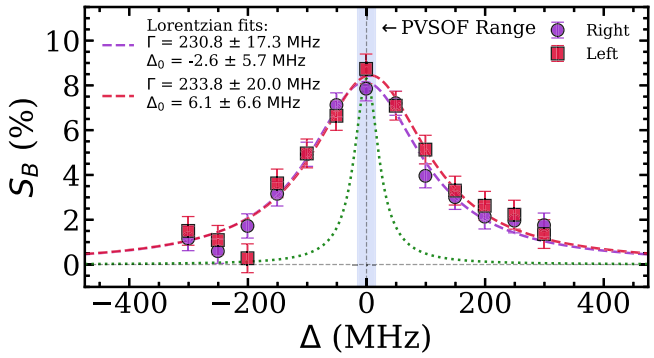


FIG. 5. Single waveguide line shapes of the $2\,^3S_1 \rightarrow 2\,^3P_2$ transition measured using left and right antennas of WG1. The mean centroid value is 8628.46 ± 4.36 MHz, in broad agreement with the Zeeman shifted transition frequency. The dotted curve is a Lorentzian function with an FWHM of ≈50 MHz corresponding to the natural linewidth. The shaded vertical bar represents the frequency detuning range used in the PVSOF measurements.

comparable to all previous measurements. The current result is shown in Fig. 4 along with previous determinations using Rabi spectroscopy from groups at Brandeis [24], Michigan [25], Mainz [26], and UCL [8].

For comparison, spectral line shapes determined from Rabi measurements using only a single waveguide (WG1) were recorded and are shown in Fig. 5. Line shapes were recorded using the left (L) and right (R) antennas corresponding to microwave radiation propagating in the $+x$ and $-x$ directions, respectively (see Fig. 1). We note that the intensity of the microwave radiation in the tuned waveguides is not expected to be constant over the large frequency range used for these measurements, and the line shapes are therefore not reliable indicators of the line centers. Lorentzian fits to the data were used to obtain estimates of the linewidths, as indicated in the legend of Fig. 5. These data were recorded using the same beam parameters used in the PVSOF measurements and therefore exhibit significant transit-time broadening [27], with a measured average width of ≈230 MHz. Ordinarily, one would not use such a fast beam for Rabi measurements, but even for much slower beams the linewidth would still be limited by the ≈50 MHz natural width, which is indicated by the dotted Lorentzian curve shown in the figure. Also shown is the frequency detuning range used in the PVSOF measurements, which clearly extends over a much smaller range than is required by Rabi line shape measurements; this is the main advantage of the PVSOF method. With improved statistics, it would be possible to perform PVSOF measurements over an even smaller frequency range.

We have demonstrated that the PVSOF method [14] can be used to measure the Ps fine structure. The experiment we describe here constitutes the first explicitly phase-sensitive measurement involving Ps, and opens the door to significant increases in precision. The main limitation of the current measurements is the low beam intensity, meaning that the experiment is limited by statistical errors. The individual phase scans (see Fig. 3) were recorded over ≈100 h of live acquisition time each. This is because we have a low positron beam rate ($\approx 10^5$/s) coupled with low Ps^* production efficiency, resulting in a Ps^* count rate of ≈2/s obtained using a ^{22}Na positron source activity of ≈200 MBq. This could be immediately improved by at least an order of magnitude using a new source with an activity of 1.85 GBq (the highest activity commercially available [28]) or by performing experiments at an intense beam facility (e.g., the NEPOMUC reactor beam in Munich [29]). An increased beam intensity would open up the possibility to use a remoderated positron beam [30], which would have a smaller spatial extent and energy spread. This would not only improve the contrast of the interference signal but would also allow the Ps^* production to be optimized [20].

Improved statistical precision would render systematic effects more significant: The Zeeman shift can be easily eliminated by terminating the magnetic field and enclosing the waveguides in a mu-metal shield, and Doppler effects can be directly observed by reversing the direction of propagation of the microwave radiation. Various modifications to the rf system could also be made, such as generating standing waves rather than the traveling waves, including probes to check for residual phase shifts or installing a rotatable waveguide assembly that would allow the Ps^* beam to encounter the rf fields in reverse order, allowing residual phase shifts to be eliminated (see, for example, Ref. [31] for a detailed discussion of these types of systematic effects).

The successful application of the PVSOF technique is the first step toward achieving a Ps measurement using the more sophisticated frequency-offset SOF (FOSOF) method [15]; this has been used for precision measurements of the

hydrogen Lamb shift (3 ppm) [31] and helium fine structure ($\lesssim 2$ ppb) [32,33], and has also been applied to measurements of the neutron gyromagnetic moment as a way to characterize magnetic fields [34]. The FOSOF technique uses separated oscillatory fields with a small frequency offset, causing the relative phase to change continuously. The resulting atomic signal oscillates in time with a phase relative to the beat signal of the two frequencies that depends on detuning from resonance. This method can potentially be used to obtain a precision much lower than the current 80 kHz precision of the QED calculations, but a more intense beam will be required both to investigate the details of PVSOF systematic effects, and to establish the feasibility of performing Ps^* FOSOF measurements.

Acknowledgments—We gratefully acknowledge T. J. Babij, J. Breeze, M. Fleck, and A. C. Vutha for helpful discussions, and J. Dumper, F. Noyes, and R. Jawad for technical assistance. This work was supported in part by the EPSRC under Grant No. EP/W032023/1.

Data availability—The data that support the findings of this article are not publicly available. The data are available from the authors upon reasonable request.

[1] W. Bernreuther and O. Nachtmann, Weak interaction effects in positronium, Z. Phys. C **11**, 235 (1981).
[2] S. G. Karshenboim, Precision study of positronium: Testing bound state QED theory, Int. J. Mod. Phys. A **19**, 3879 (2004).
[3] M. S. Safronova, D. Budker, D. DeMille, Derek F. Jackson Kimball, A. Derevianko, and C. W. Clark, Search for new physics with atoms and molecules, Rev. Mod. Phys. **90**, 025008 (2018).
[4] G. S. Adkins, D. B. Cassidy, and J. Pérez-Ríos, Precision spectroscopy of positronium: Testing bound-state qed theory and the search for physics beyond the standard model, Phys. Rep. **975**, 1 (2022).
[5] G. S. Adkins, Higher order corrections to positronium energy levels, J. Phys. Conf. Ser. **1138**, 012005 (2018).
[6] M. I. Eides and V. A. Shelyuto, Three-loop corrections to the lamb shift in muonium and positronium, Phys. Rev. A **105**, 012803 (2022).
[7] L. Gurung, T. J. Babij, S. D. Hogan, and D. B. Cassidy, Precision microwave spectroscopy of the positronium $n = 2$ fine structure, Phys. Rev. Lett. **125**, 073002 (2020).
[8] R. E. Sheldon, T. J. Babij, S. H. Reeder, S. D. Hogan, and D. B. Cassidy, Precision microwave spectroscopy of the positronium $2^3S_1 \rightarrow 2\,^3P_2$ interval, Phys. Rev. Lett. **131**, 043001 (2023).
[9] L. Gurung, T. J. Babij, J. Pérez-Ríos, S. D. Hogan, and D. B. Cassidy, Observation of asymmetric line shapes in precision microwave spectroscopy of the positronium $2\,^2S_1 \rightarrow 2^3P_J$ ($j = 1, 2$) fine-structure intervals, Phys. Rev. A **103**, 042805 (2021).
[10] R. E. Sheldon, T. J. Babij, S. H. Reeder, S. D. Hogan, and D. B. Cassidy, Microwave spectroscopy of positronium atoms in free space, Phys. Rev. A **107**, 042810 (2023).
[11] R. J. Daly, R. E. Sheldon, and D. B. Cassidy, Measurement of the fluorescence decay rate of $2\,^3P_J$ positronium, Phys. Rev. A **110**, 022807 (2024).
[12] Norman F. Ramsey, A new molecular beam resonance method, Phys. Rev. **76**, 996 (1949).
[13] C. W. Fabjan and F. M. Pipkin, Resonance-narrowed-lamb-shift measurement in hydrogen, $n = 3$, Phys. Rev. A **6**, 556 (1972).
[14] H. A. Klein, E. W. Hagley, P. K. Majumder, F. M. Pipkin, and M. E. Poitzsch, Phase-variation technique for measurement of the $n = 2$ lamb shift in he^+ using separated oscillatory fields, Phys. Rev. A **36**, 3494 (1987).
[15] A. C. Vutha and E. A. Hessels, Frequency-offset separated oscillatory fields, Phys. Rev. A **92**, 052504 (2015).
[16] L. Liszkay, C. Corbel, P. Perez, P. Desgardin, M. F. Barthe, T. Ohdaira, R. Suzuki, P. Crivelli, U. Gendotti, A. Rubbia, M. Etienne, and A. Walcarius, Positronium reemission yield from mesostructured silica films, Appl. Phys. Lett. **92**, 063114 (2008).
[17] D. B. Cassidy, Experimental progress in positronium laser physics, Eur. Phys. J. D **72**, 53 (2018).
[18] T. J. Babij and D. B. Cassidy, Positronium microwave spectroscopy using Ramsey interferometry, Eur. Phys. J. D **76**, 121 (2022).
[19] D. J. Murtagh, D. A. Cooke, and G. Laricchia, Excited-state positronium formation from helium, argon, and xenon, Phys. Rev. Lett. **102**, 133202 (2009).
[20] D. M. Newson, T. J. Babij, and D. B. Cassidy, An energy tunable continuous $2\,^3S_1$ positronium beam, Rev. Sci. Instrum. **94**, 083201 (2023).
[21] Andrzej Czarnecki, Kirill Melnikov, and Alexander Yelkhovsky, Positronium S-state spectrum: Analytic results at $o(m\alpha^6)$, Phys. Rev. A **59**, 4316 (1999).
[22] D. M. Newson and D. B. Cassidy, Measurement of the spin polarization of a slow positron beam using circularly polarized microwave radiation, Phys. Rev. Lett. **133**, 233004 (2024).
[23] L. A. Akopyan, T. J. Babij, K. Lakhmanskiy, D. B. Cassidy, and A. Matveev, Line-shape modeling in microwave spectroscopy of the positronium $n = 2$ fine-structure intervals, Phys. Rev. A **104**, 062810 (2021).
[24] A. P. Mills, Jr., S. Berko, and K. F. Canter, Fine-structure measurement in the first excited state of positronium, Phys. Rev. Lett. **34**, 1541 (1975).
[25] S. Hatamian, R. S. Conti, and A. Rich, Measurements of the $2\,^3S_1$-$2\,^3P_J$ ($J = 0$, 1, 2) fine-structure splittings in positronium, Phys. Rev. Lett. **58**, 1833 (1987).
[26] D. Hagena, R. Ley, D. Weil, G. Werth, W. Arnold, and H. Schneider, Precise measurement of $n = 2$ positronium fine-structure intervals, Phys. Rev. Lett. **71**, 2887 (1993).
[27] W. Demtröder, *Laser Spectroscopy*, 3rd ed. (Springer, New York, 2003).
[28] T. N van der Walt and C. Vermeulen, Thick targets for the production of some radionuclides and the chemical processing of these targets at Ithemba labs, Nucl. Instrum. Methods Phys. Res., Sect. A **521**, 171 (2004).

[29] C. Hugenschmidt, C. Piochacz, M. Reiner, and K. Schreckenbach, The NEPOMUC upgrade and advanced positron beam experiments, New J. Phys. **14**, 055027 (2012).
[30] A. P. Mills, Jr., Brightness enhancement of slow positron beams, Appl. Phys. **23**, 189 (1980).
[31] N. Bezginov, T. Valdez, M. Horbatsch, A. Marsman, A. C. Vutha, and E. A. Hessels, A measurement of the atomic hydrogen lamb shift and the proton charge radius, Science **365**, 1007 (2019).
[32] K. Kato, T. D. G. Skinner, and E. A. Hessels, Ultrahigh-precision measurement of the $n = 2$ triplet p fine structure of atomic helium using frequency-offset separated oscillatory fields, Phys. Rev. Lett. **121**, 143002 (2018).
[33] F. Heydarizadmotlagh, T. D. G. Skinner, K. Kato, M. C. George, and E. A. Hessels, Precision measurement of the $n = 2$ triplet P $J = 1$ to $J = 0$ fine structure of atomic helium using frequency-offset separated oscillatory fields, Phys. Rev. Lett. **132**, 163001 (2024).
[34] A. Fratangelo, P. Heil, C. Klauser, G. Markaj, M. Persoz, C. Pistillo, I. Schulthess, J. Thorne, and F. M. Piegsa, Frequency-offset separated oscillatory fields technique applied to neutrons, Phys. Rev. C **109**, 065503 (2024).